

RESIDUAL STRESS MODELLING OF PIPE BENDS

Siavash Khajehpour¹⁾ and Metin Yetisir¹⁾

1) Atomic Energy of Canada Limited

ABSTRACT

In one CANDU® nuclear station, 11 outlet feeder pipes have been replaced because of cracking in the bends. After the first two leak-before-break failures, nine feeders with cracks were detected by inspection and removed from service. In all cases, cracks were axial and coincident with regions of high tensile residual stresses, indicating that the residual stress had a significant role in these failures. These cracks occurred in tight-radius pipe bends, i.e. bends with a small value of bend radius (r) to pipe diameter (D) ratio, $r/D = 1.5$. However, large-radius feeder bends with $r/D > 4$ were also exposed to the same operating and environmental conditions as tight-radius bends and, hence, were considered for crack susceptibility. To evaluate the relative crack susceptibility of large-radius pipe bends to that of the tight-radius pipe bends, a detailed evaluation of residual stresses was needed.

In this paper, results of numerical simulations of a large-radius feeder bend are presented. This feeder bend was selected for the simulations, because it was previously studied experimentally and detailed information on residual stresses, wall thickness, cross-sectional shape and plastic deformation at two bend cross-sections were documented. The predicted residual stress, plastic deformation, cross-sectional shape and wall thickness values are compared to those obtained using the experimental data.

INTRODUCTION

CANDU nuclear reactors are pressurized heavy water reactors based on fuel channel design. Feeders connect the in-reactor fuel channels with the large-diameter primary heat transport pipes. In a typical feeder, there are a number of bends and welds, which are potential locations of high residual stresses. Examinations of cracked feeder bends and measurements of residual stresses revealed that the cracks were associated with the locations of high residual stress, suggesting that residual stress had a major role in these failures [1]. A significant amount of CANDU feeder bend residual stress data has been generated since 1997 using neutron diffraction measurements [2], [3]. The information regarding the magnitude and distribution of residual stresses in feeder bends has been used to identify possible crack locations, to evaluate susceptibility to cracking of various feeder bends and to develop inspection strategies in limited-scope inspection campaigns. However, information obtained using experimental techniques is geometry dependent, expensive and limited to the locations of measurement points. Hence, an analytical or numerical model for feeder bend residual stresses could be a valuable tool to supplement experimental data.

BEND GEOMETRY

In CANDU stations, feeder pipes range from 1.5 to 3.5 inches in nominal pipe diameter and are fabricated from SA-106 Grade B material. Each feeder pipe contains up to seven bends, either large-radius bends with a 12- or 15-inch bend radius, or tight-radius bends with a 3 inch or 3.75 inch bend radius. Tight-radius bends use a bend radius that is 1.5 times the Nominal Pipe Size (NPS), i.e., $r/D = 1.5$ where r is the bend radius and D is the nominal pipe diameter. In large-radius bends the r/D ratio is larger than 4.0. For the specific example in this report, the numerical model was developed for a large-radius feeder bend with $r/D = 4.3$.

SIMULATION OF PIPE BENDING PROCESS

In order to provide estimates of residual stress arising from cold bending of these feeder pipes for a fitness-for-service study [2], [3], a series of simulations were undertaken to calculate the residual stresses and plastic strains in a large-radius feeder bend. The manufacturing process was modeled using the H3DMAP¹ hybrid explicit solution module, since this provides for automatic spring back once the clamp and die are released. This is a necessary feature to ensure accuracy of residual stress results. The three steps of the bending process, namely, 1) clamping, 2) bending, and 3) releasing the tube, were modeled using an explicit solution technique. The intention was to follow the manufacturing process as closely as possible. The selected large-radius bend is a 3.5 inch NPS expanded section of an outlet feeder connecting to the outlet header. It is bent by 108° and has the smallest bend radius-over-feeder diameter ratio ($r/D = 4.3$) among all large-radius

® CANDU (CANadian Deuterium Uranium) is a registered trademark of Atomic Energy of Canada Limited (AECL).

¹ An in-house Non-Linear Finite Element Program.

bends [3]. Hence, the selected 3.5 inch NPS bend is considered to be the limiting large-radius feeder bend from a residual stress point-of-view. The key elements of the simulation model representing the actual fabrication tool and die set up are given in Figure 1.

Bending Mechanism Assembly

The bending setup for the large-radius bend is comprised of a rotary die, a clamp and a pressure die (Figure 1). The rotary die consists of a straight portion that is 304.8 mm (12") long and is used for grabbing the feeder pipe for bending. The circular part of the rotary die has a radius of 375.5 mm ($14\frac{25}{32}$ ") from the centre of rotation to the outmost external part of the die. The cross section of the rotary die (both straight and circular parts) is a semi circle (180°) with a radius of 50.597 mm, which is slightly less than the outside radius of the pipe. The clamp is a straight piece that is 304.8 mm (12") long and has a cross section that is comprised of a 173.27° circular arc with a radius that is identical to that of the rotary die. On the inside surface of the clamp, a series of ridges is machined to provide a better grip on the pipe and to prevent slippage between pipe and clamp. The pressure die is 1117.8 mm (44") long. It has the same circular cross-section as the clamp. After the pipe is clamped, the remaining gap between the clamp and rotary die is approximately 0.813 mm (0.032"). The initial gap between the clamp and pressure die is 1.651 mm (0.065").

Modelling Assumptions

In order to model the bending process as accurately as possible the following details are considered in the simulation model:

- To exploit symmetry in the problem, only the top half of the pipe, rotary die, clamp and pressure die are modeled.
- The pipe is modeled using 3D nonlinear hexahedron elements. Four and twenty-four divisions through the thickness and circumferentially are considered, respectively. The pipe mesh is axially refined in order to capture the axial residual stresses accurately.
- The clamp, rotary die and pressure die are modeled using rigid 3D shell elements. The meshing of these components are finer than the pipe in both the axial and circumferential directions in order to prevent any local concentration of contact/friction forces and to ensure that the final cross-sectional shape of the bent pipe resembles the actual cross sectional dimension of the rotary die.
- Symmetric treatment on contact pairs is employed to eliminate the possible complications of contact penetrations.
- Since the clamping force is displacement driven, a series of beam elements is used to connect the clamp to the rotary die. The clamping process was simulated by enforcing the axial strain in the beam elements using an artificial thermal strain (cooling) such that the desired distance between the rotary die and clamp is achieved. Conversely, the unclamping is achieved using an artificial thermal strain (heating) releasing the clamp.
- After bending and unclamping steps, it was observed that the pipe remains stuck in the rotary die due to friction. This is consistent with the observations made during the manufacturing process. For a complete release, the restart capability was used where the contact elements are removed and the simulation is restarted.
- The unclamping process achieved through artificial thermal strain and releasing of the pipe by means of the restart capability in H3DMAP allows the pipe to spring back and arrive at its final stage of the bending process.
- Since the clamp has a series of circumferential ridges to provide a better grip on the pipe, an artificially high friction factor of 8 was used for the clamp-to-pipe interface. The high coefficient of friction simulates the effect of machined ridges in the clamp by preventing the pipe from sliding between the clamp and the rotary die. For the pipe-to-rotary die interface, a friction factor of 0.4 is used. This value is considered typical for machined steel-to-steel surfaces [4]. A small friction factor of 0.1 for the pressure die and pipe interface is assumed, because the pressure die moves together with the pipe (i.e., no relative motion in the axial direction) as the pipe is bent (see Figure 1). Hence, this value has very little impact on the simulation results.
- The rotary die is rotated around the centre of rotation after the clamping process is completed. Since the clamp is connected to the die by beam elements, the clamp is moved with the same rotational velocity around the same centre while beam elements keep the relative distance between the rotary die and clamp constant. At this point, the pipe moves with the clamp and the rotary die due to perpendicular and tangential (i.e., friction force) contact forces between the pipe/die and the pipe/clamp.
- As the rotary die starts rotating around the centre of rotation, the pressure die moves along the length of the pipe with the same tangential velocity of the outer radius as the die and provides the pipe with lateral support.
- Ongoing testing programs using actual feeder materials indicate some variation in the stress/strain curves for axial, hoop and radial directions. This directional variation of material properties is not modelled in the present study.

The H3DMAP hybrid explicit solution method was used for the simulations. A sensitivity analysis on the number of simulation cycles was performed to establish the minimum reasonable number of cycles that results in a converged solution.

Numerical Model

Given the complexity of the model, a variety of element types are used for each of the structural components. These elements are listed in Table 1. In the simulations, the pipe is initially assumed stress-free. Kinematic boundary conditions introduced by the movement of the clamp, pressure die and rotary die result in contact forces at the contact surfaces. These forces are internally calculated by H3DMAP and are applied to the pipe to simulate the bending process.

Table 1
Details of Simulation Model Topology

Model Details		
Component	Element Type	Number of Elements
Pipe	3D Continuum	9,024
Clamp	3D Rigid Shell	576
Die	3D Rigid Shell	2,976
Pressure Die	3D Rigid Shell	1,920
Clamping Beams	3D Beam	48
Contact Pairs	Contact	12 (symmetric treatment)
Total Number of Elements		14,544
Total Number of Nodal Points		17,650

The clamp, die, pressure die and clamping beams are explicitly modelled (Figure 1) according to the dimensions provided by the manufacturer. The constitutive model used for these components is an elastic material with the following parameters; density = 7800 kg/m^3 , Poisson's ratio = 0.3, and modulus of elasticity = 200 GPa.

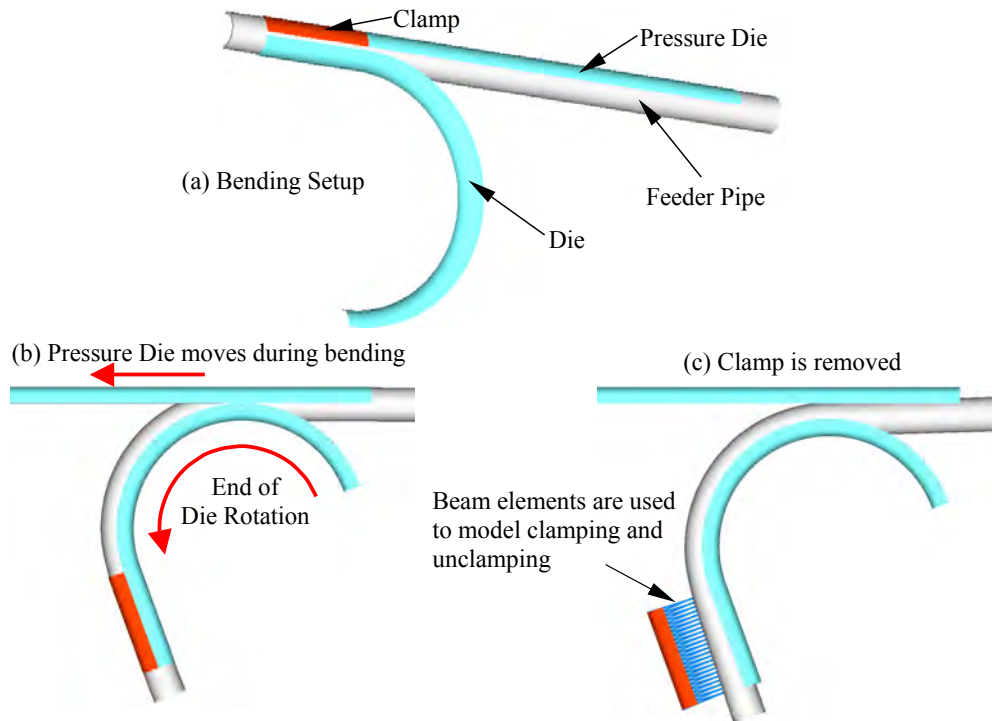


Figure 1 Feeder Bend Simulation Model

Feeder Pipe Material Model

For this material, an elastic-plastic isotropic hardening model is considered (Figure 2). The curve denoted as U575 in Figure 2 is measured using samples from the straight section of a feeder bend as part of the feeder fitness-for-service program funded by CANDU Owners Group (COG). This material model is used as a baseline case in all simulations unless otherwise stated. To parametrically study the effect of material properties on the results, additional simulations were conducted using assumed material properties denoted as U775 and U475 in Figure 2. The names of the material models come from the value of the ultimate strengths, i.e. 475 MPa, 575 MPa and 775 MPa, at 15% strain. The density of the feeder pipe is input as 7800 kg/m^3 and Poisson's ratio as 0.3.

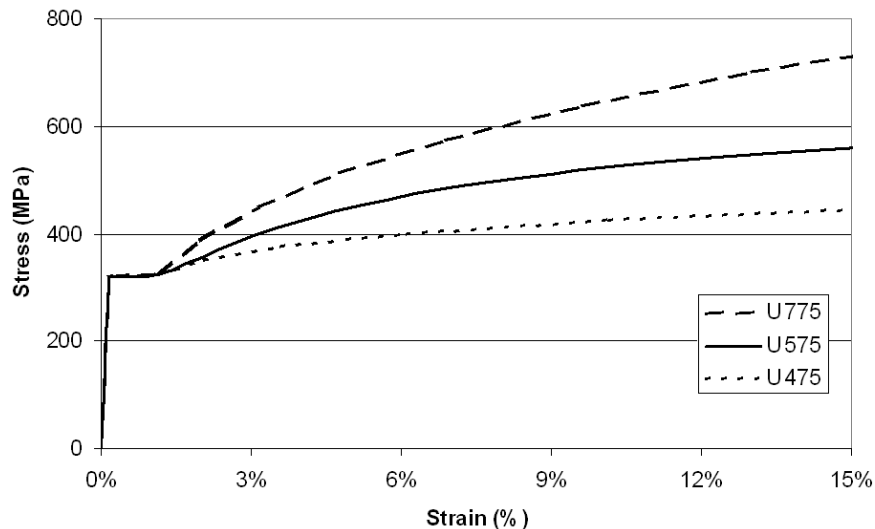


Figure 2 Stress-Strain Curves Considered for the Feeder Pipe

SIMULATION RESULTS AND COMPARISON

The geometric factors that have a significant influence on the results are the rotary die, the clamp and the pressure die dimensions. The cross sections (e.g., radius) of these components are slightly smaller than that of the feeder pipe. In addition, none of these components is a full semi-circle. Therefore, slight deviations in the actual dimensions of the feeder pipe, tool and die will affect the magnitude and distribution of the residual stresses. To reduce uncertainties in the analyses, the dimensional information of the dies and the clamp was obtained from the manufacturer of the feeder bend used in the comparison study. Another important factor is the assumption regarding the clamping of the pipe. It is critical to model the clamp-to-rotary die interface in the same manner as in the manufacturing set up. To accommodate the high level of axial friction between the clamp and the rotary die introduced by the circumferential grooves in the clamp, an artificially high friction factor of eight is assumed. The assumption that the pressure die moves toward the die by the same amount as the clamp as well as the friction model/factors chosen between the die and the pipe also have some influence on the results.

Material properties have a significant effect on residual stress predictions. However, the kinematic variables such as displacement and the resulting plastic strain components in the hoop and axial directions are observed to be less sensitive to the material assumptions. This is because the plastic strains are directly related to the overall dimensions of the die and the speed at which the bending is performed. As a result, it was observed that the material work hardening behaviour has a greater effect on residual stresses than on the plastic strain.

The bent pipe for which the simulation of the bending process is performed is shown in Figure 3. The measurements given in [3] consist of axial and hoop plastic strains of the bent pipe on the outside surface in addition to stresses that are measured for Sections A and B, 1 mm from the outside and inside surfaces of the pipe. It should also be noted that locations (circumferential angle) where the results from simulations are reported refer to the angle where the elements were located before the pipe was bent. However, the measurement locations (circumferential angles) are with respect to the deformed geometry of the pipe. The magnitude of the location offset between measurements and simulation results is not exactly known but it is assumed not to be significant.

Comparison of Axial and Hoop Stresses

In Figure 4, the comparison between simulation results and measurements for axial and hoop stresses at 1 mm from the outer surface for Sections A and B are given. For the axial and hoop residual stress measurements, neutron diffraction was used. In order to provide a proper comparison, the measurement uncertainty bands are included in the comparison plots. As observed in Figure 4, the agreement between the measured and predicted hoop residual stresses is acceptable considering the uncertainty in the measurements. For the axial residual stress, the comparison is not quite as good. However, the distribution is predicted quite well, with the magnitudes in tension and compression falling somewhat outside the measurement bands. This behaviour follows from the greater differences in work hardening behaviour at the higher strains observed in the axial direction. From further examination of the data, it appears that the calculated stresses on the ID surface are smoother than the calculated stresses on the OD surface. This may be due to the friction forces between the pipe and the rotary die affecting the stresses in proximity of the OD surface.



Figure 3 Bent Feeder Pipe [3]

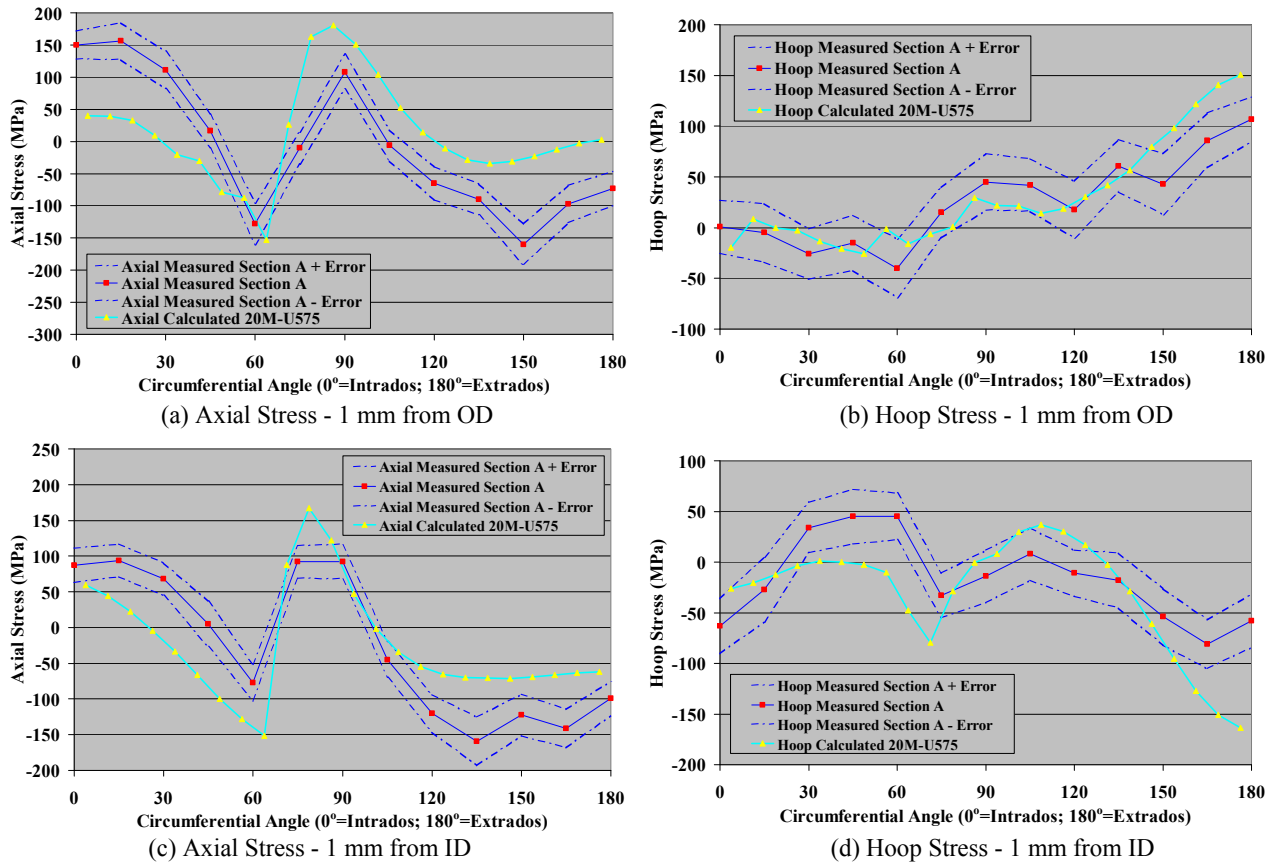


Figure 4 Comparisons of the Axial and Hoop Stresses as a Function of Circumferential Angle at Apex

Comparison of Plastic Deformations

The plastic strains obtained from simulations for different material properties of U775, U575 and U475 are also compared with measurements. The calculated plastic strains for different material properties are very similar. This can be attributed to the fact that the overall deformation is more dependent on the overall geometry of the bend radius. In Figure 5 the predicted plastic strains for the U575 material model is compared with measurement. It was found that the predicted plastic strain distribution match the measurements very well with axial plastic strains ranging from -11% to 17% (measured range was -12 to 15%) and the hoop plastic strains ranging from -10% to 4% (measured range was -9% to 5%)

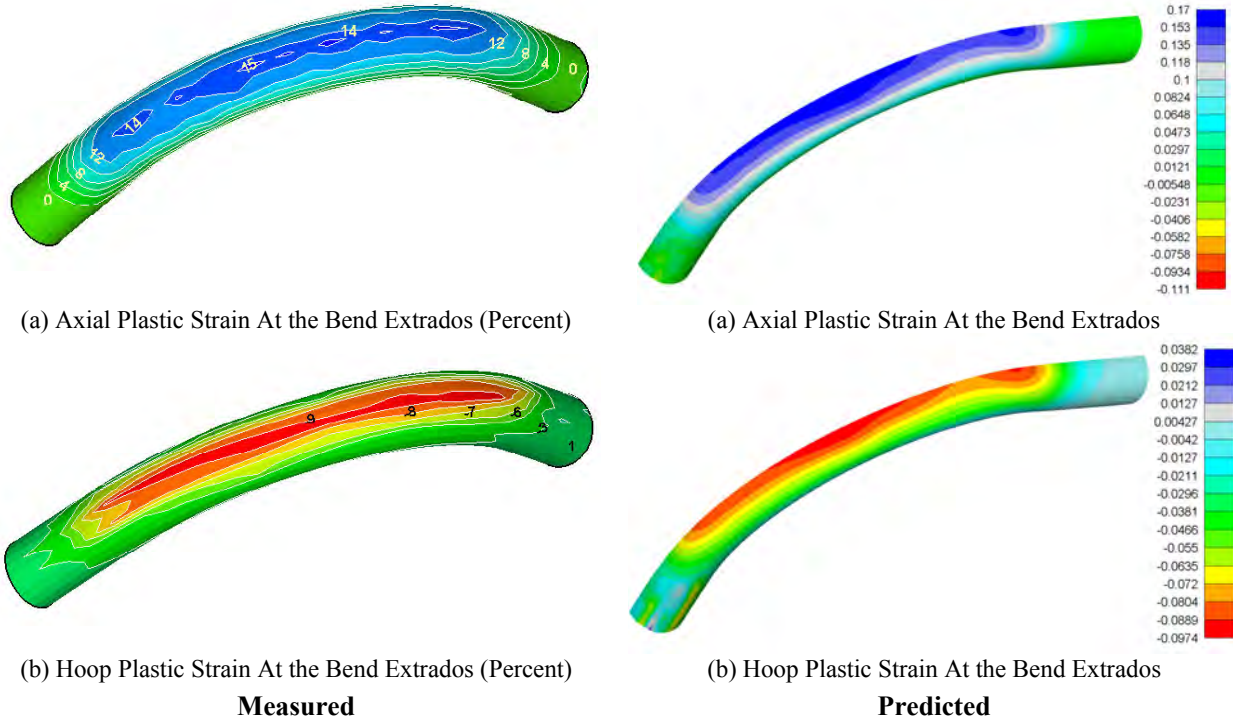


Figure 5 Comparisons of Measured and Predicted Plastic Strains – Material U575

Effect of Material Properties

Stresses obtained from simulations, however similar in shape, differ in magnitude when comparing simulation results for different material properties. Comparison between simulation results and measurements for axial and hoop stresses at 1 mm from outer and inner surfaces for different material properties shows that the result of the simulation for material U775 predicts higher tensile and compressive stresses in the body of the pipe whereas the magnitude of the maximum tensile and compressive stresses obtained for material U475 is less compared to material U575 (these results are not presented in this paper). Since the overall plastic deformation is virtually the same for all three material properties, before the release of the clamp, stresses in the pipe differ quite significantly for different material properties. However, the same modulus of elasticity and almost the same amount of spring back result in approximately the same change in the state of the stress through the cross section after the clamp is released. Hence, a large uncertainty in the stress-strain material property results in a large variation (uncertainty) in the predicted magnitudes of residual stresses.

Deformed Shape at Sections A and B

The dimensional measurements of Sections A and B (diameter and thickness) in addition to the results obtained from simulations for different material properties are given in Table 2. Data presented in Table 2 demonstrate a very good agreement between measurements and simulation results. The measurements lie somewhere in between the results obtained by using material models U775 and U575. As expected the intrados pipe wall is thicker and the wall thickness on the extrados side is thinner after the bending process is finished. Also, comparison between the diametral measurements (Sections A and B) and the simulation results for vertical and horizontal components (plane of symmetry) show good agreement with measurements and lie between U775 and U575. Shown in Figure 6 are the deformed cross sections of the pipe at the bend apex (Section A) for both the simulation results (materials U775 and U575) and measurements [3].

Table 2
Comparison of Initial Pipe Dimensions and Deformed Pipe Dimensions from Simulations

Case Index		Wall Thickness (m)		Outside Diameter (m)		
		Extrados	Intrados	Vertical	Horizontal	
Original		0.00808	0.00808	0.1016	0.1016	
FE Analysis	U775 Section A	0.00755	0.00852	0.1013	0.0977	
	U575	Section A	0.00747	0.00853	0.1012	0.0965
		Section B	0.00745	0.00855	0.1012	0.0963
U475	Section A	0.00737	0.00855	0.1011	0.0952	
Measured [3]	Section A	0.0075± 0.0002	0.0083± 0.0002	0.1014± 0.0002	0.0977± 0.0002	
	Section B	0.0076± 0.0002	0.0083± 0.0002	0.1016± 0.0002	0.0976± 0.0002	

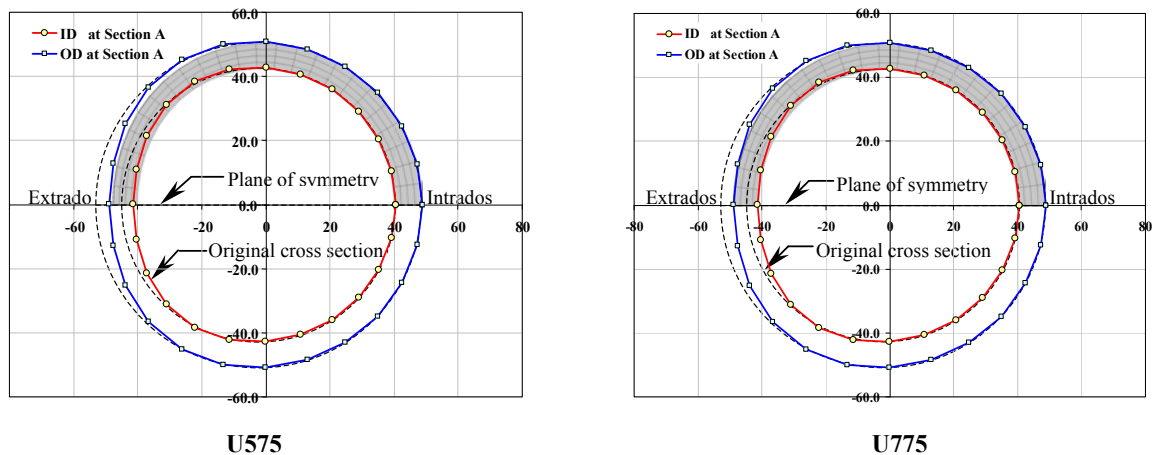


Figure 6 Comparison of Measured and Calculated Cross-Section at the Apex (Section A)

CONCLUSIONS

Based on the residual stress measurements [2][3] and simulations performed in support of this study, the following are concluded:

- **Residual Stresses:** Good agreement is obtained between the predicted and measured residual stresses when the U575 material property is used. This material model is developed from the measurements using an actual feeder material.
- **Plastic Strains:** The plastic strains obtained from simulations are in very good agreement with measurements. This result is valid regardless of the material properties. This can be attributed to the fact that the overall deformation is more dependent on the geometry of the feeder pipe and the bend radius, and less dependent on the material properties of the pipe.
- **Wall-thickness and Ovality:** The predicted change in the cross-sectional shape, i.e., bend ovality, agrees very well with the measurements. The predicted thinning of the wall on the extrados side and thickening of the pipe wall on the intrados side also compare very well with the measurements.

The results of this study indicate that the numerical models can be used to successfully model the bending process of feeder bends. The trends in the parametric studies indicate that, further improvements are likely in the predicted results. These models can be used to quantify residual stresses in various feeder bends with differing geometries, such as those with different feeder diameters, bend angles, and bend radii and proximately to another bend. Numerical models can also be used to answer questions, such as the effect of various parameters used in the manufacturing process, the effect of wall thinning on residual stress distribution, the extent of residual stresses beyond the bend region, the combined effects of residual and service stresses, and the provision of input for crack stability analyses.

ACKNOWLEDGEMENTS

The presented work was part of a package funded by the Feeder Integrity Joint Project (FIJP) of CANDU Owners Group (COG). The contribution and the permission of the utilities to publish this paper are deeply appreciated.

REFERENCES

- [1] Slade, J.P.; Gendron, T.S., “Flow Accelerated Corrosion and Cracking of Carbon Steel Piping in Primary Water – Operating Experience at the Point Lepreau Generating Station”, 12th International Conference on Environmental Degradation of Materials in Nuclear Power Systems-Water Reactors, Salt Lake City, USA, 2005 August.
- [2] Yetisir, M.; Rogge, R.; Donaberger, R., “The Effect of Manufacturing Process on Residual Stresses of Pipe Bends”, 2005 ASME-PVP Conference, Denver, Colorado USA, 2005 July.
- [3] Yetisir, M.; Rogge, R.; Donaberger, R., “Residual Stresses of CANDU Feeder Bends – Effect of Bend Radius”, 2006 ASME-PVP Conference, Vancouver, BC, Canada, 2006 July.
- [4] R.L. Norton, “Machine Design, An Integrated Approach”, Second Edition, Prentice Hall, 2000.